

# Preventing the Decodability Attack based Cross-matching in a Fuzzy Commitment Scheme

E.J.C. Kelkboom, J. Breebaart, T.A.M. Kevenaar, I. Buhan, R.N.J. Veldhuis

**Abstract**—Template protection techniques are used within biometric systems in order to safeguard the privacy of the system’s subjects. This protection also includes unlinkability, i.e. preventing cross-matching between two or more reference templates from the same subject across different applications. In the literature, the template protection techniques based on fuzzy commitment, also known as the code-offset construction, have recently been investigated. Recent work presented the decodability attack vulnerability facilitating cross-matching based on the protected templates and its theoretical analysis. Firstly, we extend the theoretical analysis and include the comparison between the system and cross-matching performance. We validate the presented analysis using real biometric data from the MCYT fingerprint database. Secondly, we show that applying a random bit-permutation process secures the fuzzy commitment scheme from cross-matching based on the decodability attack.

## I. INTRODUCTION

When using an application based on biometrics, first a *reference template* is generated from the biometric sample provided in the enrolment phase for later use. In the authentication phase, a new biometric sample is acquired and compared with the reference template. Hence, the application requires this reference template for a successful authentication and therefore it needs to be stored. Basically, there are two options of storage, namely on a token carried by the subjects themselves or in a centralized database. The latter case is considered to be more convenient for the subjects. However storing unprotected biometric reference templates in centralized databases for each application increases the privacy risk. For example, if these databases are compromised, an adversary could check the types of applications or services a specific subject has subscribed to. In the literature, this is known as *cross-matching*.

Therefore it is not a surprise that the ISO guidelines [1] dictate the avoidance of centralized databases if possible. Some known countermeasures to safeguard the privacy and security by enforcing some of the ISO guidelines are (i) the practice of *data separation* where the most privacy sensitive information is stored on an individual smartcard or token, (ii) the use of *data minimization* principles, (iii) the use of *classical encryption* techniques such as DES, AES, RSA to augment the confidentiality or integrity of the reference template and (iv) the implementation of *template protection* which creates irreversible, renewable and unlinkable reference

templates, i.e. protected reference templates. In our work we focus only on the template protection method.

In the literature, numerous template protection methods such as the *Fuzzy Commitment Scheme* (FCS) [2], *Helper Data System* (HDS) [3]–[5], *Fuzzy Extractors* [6], [7], *Fuzzy Vault* [8], [9] and *Cancelable Biometrics* [10] have been proposed, with the claim of preventing cross-matching. However, recently it was presented in [11] that fuzzy vaults were susceptible to cross-matching and [12] solved this issue by hardening the protected reference template using a secret key or password provided by the subject. The requirement of keeping the key or password secret however, has a serious impact on the convenience of the biometric system.

In the FCS construction, also known as the code-offset construction, the binary vector extracted from the biometric sample is XOR-ed with a randomly selected codeword resulting into auxiliary data that is stored as part of the protected template. Certain implementations of the Helper Data System, Fuzzy Extractors are based on this FCS construction. Possible cross-matching vulnerabilities for template protection systems based on the FCS construction are briefly discussed in [13] and are based on attack methods using exhaustive search. More recently, a new vulnerability known as the *decodability attack* has been published for the case when the FCS is based on a linear error-correcting codes (ECC). To the best of our knowledge, the cross-matching vulnerability of the FCS construction is first published by the presentation of Dr. Stoianov at the European Biometrics Forum (EBF) Biometric Encryption Seminar [14]. Cross-matching is made possible by simply checking whether decoding the XOR of two auxiliary data elements stored in different databases leads to a valid codeword. If it leads to a valid codeword the two auxiliary data most likely belong to the same subject and is labeled as genuine. Therefore, this vulnerability is also known as the decodability attack. More recently, a theoretical analysis is presented in [15] where the authors determine the probability that the decodability attack incorrectly labels two auxiliary data from different subjects as genuine under the assumption that across the whole population the bits of the binary vector are independent and uniform.

**Contributions:** As our first contribution, we extend the theoretical analysis from [15] and show the relationship between the cross-matching performance with the template protection system performance itself. Furthermore, we empirically evaluate the theoretical analysis using real biometric data from the MCYT fingerprint database and show that if no care is taken cross-matching based on the decodability attack is indeed possible. However, as our second contribution we will show that this vulnerability can be prevented by implementing a bit-permutation or shuffling randomization process on the binary

E.J.C. Kelkboom, J. Breebaart, and Ileana Buhan are with Philips Research, The Netherlands {Emile.Kelkboom, Jeroen.Breebaart, Ileana.Buhan}@philips.com

T.A.M. Kevenaar is with priv-ID, The Netherlands Tom.Kevenaar@priv-id.com

R.N.J. Veldhuis is with the University of Twente, Fac. EEMCS, The Netherlands R.N.J.Veldhuis@utwente.nl

vector. Consequently, the cross-matching performance is close to random.

The outline of this paper is as follows. In Section II we briefly describe the FCS construction, present the properties of a linear error-correcting code (ECC), and discuss a probability estimation case extensively used in the remainder of this work. In Section III we discuss the possible cross-matching attacks including the newly published decodability attack [14], [15]. In Section IV we theoretically analyze both the cross-matching and template protection system performance and show their relationship. Validation of the theoretical performances are conducted in Section V using the MCYT fingerprint database. In Section VI we show that a bit-permutation randomization process reduces the effectiveness of the decodability attack. Conclusions are given in Section VII.

## II. PRELIMINARIES

The template protection scheme under consideration is known as the Fuzzy Commitment Scheme (FCS) from [2] and is based on an error-correcting code (ECC). We first discuss the notations related to the ECC and thereafter we present the FCS. Furthermore, we discuss the estimation of the probability mass function (pmf) of the number of bit errors when XOR-ing two random binary vectors, which is extensively used in the remainder of this work.

### A. Linear Error-Correcting Code

We denote a  $t_c$ -error linear binary error-correcting code as  $[n_c, k_c, t_c]$ , where  $n_c$  is the length of the codeword  $\mathbf{C}$ ,  $k_c$  the length of the message or key  $\mathbf{K}$ , and  $t_c$  the error-correcting capability.

The *ECC Encoder (Enc)* function converts the key  $\mathbf{K} \in \{0, 1\}^{k_c}$  into its corresponding codeword  $\mathbf{C} \in \{0, 1\}^{n_c}$ . The codebook  $\mathcal{C}$  is the set of all valid codewords of the ECC with cardinality  $|\mathcal{C}| = 2^{k_c}$ . As the distance function we use the Hamming distance denoted as  $d_H\{\cdot, \cdot\}$  and the Hamming weight denoted as  $\|\cdot\|$ . The minimum distance of the codebook  $\mathcal{C}$  is  $d = 2t_c + 1$ , therefore it can correct up to  $t_c$  bit errors. Because of the linearity property of the ECC it holds that the XOR operation between any pair of codewords leads to another codeword from the same codebook  $\mathcal{C}$ , namely  $\forall \mathbf{C}_i, \mathbf{C}_j \in \mathcal{C} : \mathbf{C}_i \oplus \mathbf{C}_j = \mathbf{C}_k$ , with  $\mathbf{C}_k \in \mathcal{C}$ . Furthermore, we define  $W_{\mathcal{C}}$  to be the set of possible weights  $w$  of the codewords from  $\mathcal{C}$ , while the function  $N_{\mathcal{C}}(w)$  returns the number of codewords  $n_w$  with weight  $w$ , with  $\sum_{w \in W_{\mathcal{C}}} N_{\mathcal{C}}(w) = |\mathcal{C}|$ .

Given a word  $\mathbf{w} \in \{0, 1\}^{n_c}$  and the smallest distance to any codeword defined as  $d_c(\mathbf{w}, \mathcal{C}) \stackrel{\text{def}}{=} \min_{\mathbf{C} \in \mathcal{C}} d_H(\mathbf{w}, \mathbf{C})$ , the *ECC Decoder (Dec)* function returns the key corresponding to the closest codeword from the codebook  $\mathcal{C}$  if the smallest distance  $d_c(\mathbf{w}, \mathcal{C})$  is smaller than or equal to the error-correcting capability  $t_c$ , i.e.  $d_c(\mathbf{w}, \mathcal{C}) \leq t_c$ . When the smallest distance is larger than the error-correcting capability,  $d_c(\mathbf{w}, \mathcal{C}) > t_c$ , then the word is not decodable and the *ECC Decoder* function either returns a decoding error or randomly selects a key.

In our experiments we use the linear block type ECC ‘‘Bose, Ray-Chaudhuri, Hocquenghem’’ (BCH), with some  $[n_c, k_c, t_c]$

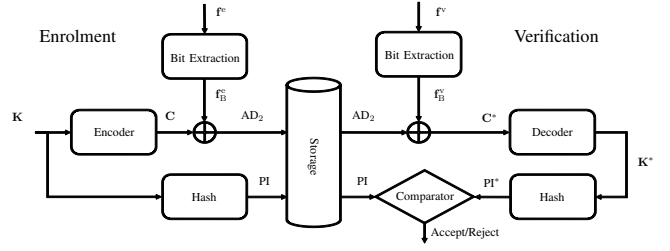


Fig. 1. The fuzzy commitment scheme (FCS) combined with a bit extraction module.

settings given in Table I. For the BCH ECC we use the maximum error-correcting capability  $t_c^*$  is limited to around 25% of the codeword size  $n_c$  (see Table I), and if the word is not decodable it outputs the first  $k_c$  bits of the word as the key.

### B. Fuzzy Commitment Scheme

The fuzzy commitment scheme (FCS) from [2] is one of the first template protection techniques and is based on the *bit commitment technique* known within the field of cryptography. The FCS works on discrete biometric data, while in practice most biometric data are continuous. Fig. 1 portrays the FCS construction combined with a bit extraction module.

In the enrolment phase the real-valued column *feature vector*  $\mathbf{f}^e \in \mathbb{R}^{N_F}$  is extracted from each  $N_e$  biometric enrolment sample by the feature extraction algorithm. From the  $N_e$  feature vectors, a single binary column vector  $\mathbf{f}_B^e \in \{0, 1\}^{N_F}$  is created. For each component, we extract a single bit using a bit extraction scheme based on thresholding, where the mean of the background density is chosen as the threshold and estimated from a disjoint training set [3], [4], [16]. Prior to thresholding the mean of the  $N_e$  feature vectors is taken. Furthermore, a random key  $\mathbf{K} \in \{0, 1\}^{k_c}$  is created and encoded by the *ECC Encoder* module into a codeword  $\mathbf{C} \in \{0, 1\}^{n_c}$  from  $\mathcal{C}$ . The fundamental property of the FCS is the XOR operation of the codeword  $\mathbf{C}$  and the binary vector  $\mathbf{f}_B^e$  creating the offset  $\mathbf{AD}_2$  as helper data,  $\mathbf{AD}_2 = \mathbf{C} \oplus \mathbf{f}_B^e$ . The helper data  $\mathbf{AD}_2$  is also referred to as the *Auxiliary Data* in [17], in line with standardization activities in ISO [1]. Together

TABLE I  
EXAMPLES OF THE BCH ECC GIVEN BY THE CODEWORD ( $n_c$ ) AND KEY ( $k_c$ ) LENGTH, THE CORRESPONDING CORRECTABLE BITS ( $t_c$ ), AND THE RELATIVE ERROR CORRECTING CAPABILITY  $t_c/n_c$ .

$n_c$ [bits]	$k_c$ [bits]	$t_c$ [bits]	$t_c/n_c$
31	6	7	22.6%
	11	5	16.1%
	16	3	9.7%
63	7	15	23.8%
	16	11	17.5%
127	24	7	11.1%
	8	31	24.4%
	22	23	18.1%
	36	15	11.8%

with the hash of  $\mathbf{K}$ , also referred to as the *Pseudonymous Identifier* (PI), we obtain the protected template. As described in [2],  $\mathbf{f}_B^e$  is equivalent to the *witness* with which we commit the codeword  $\mathbf{C}$  using the XOR operation considered to be similar to the one-time-pad encryption algorithm. The outcome of the commitment is the  $\text{AD}_2$  and PI pair, which together is also known as the *blob*.

In the verification phase, the binary vector  $\mathbf{f}_B^v$  is created by quantizing the mean of the  $N_v$  verification feature vectors  $\mathbf{f}^v$ . Hereafter, the auxiliary data  $\text{AD}_2$  is XOR-ed with  $\mathbf{f}_B^v$  resulting into the possibly corrupted codeword  $\mathbf{C}^* = \text{AD}_2 \oplus \mathbf{f}_B^v = \mathbf{C} \oplus (\mathbf{f}_B^e \oplus \mathbf{f}_B^v) = \mathbf{C} \oplus \mathbf{e}$ , where the Hamming distance  $\epsilon = d_H(\mathbf{f}_B^e, \mathbf{f}_B^v) = \|\mathbf{e}\|$  indicates the number of errors corrupting the codeword  $\mathbf{C}$ . Decoding  $\mathbf{C}^*$  by the *ECC Decoder* module leads to the candidate key  $\mathbf{K}^*$ . The candidate pseudonymous identifier  $\text{PI}^*$  is obtained by hashing  $\mathbf{K}^*$ . A match is returned by the *Comparator* module if both PI and  $\text{PI}^*$  are equal, which occurs only when  $\mathbf{K}$  and  $\mathbf{K}^*$  are equal. Both secrets are equal when the Hamming distance between the binary vectors  $\mathbf{f}_B^e$  and  $\mathbf{f}_B^v$  is smaller or equal to the error-correcting capability of the ECC,  $\epsilon = d_H(\mathbf{f}_B^e, \mathbf{f}_B^v) \leq t_c$ . Hence, to successfully decommit the blob, a new witness  $\mathbf{f}_B^v$  has to be provided that is within  $t_c$  bit differences with the original witness  $\mathbf{f}_B^e$ .

An illustration of the code-offset is presented in Fig. 2, where the  $n_c$  dimensional problem is simplified into a 2D problem. The grid of small dots represent the word space  $\{0, 1\}^{n_c}$ , while the bigger dots represents the codewords from  $\mathcal{C}$  with the error-correcting capability represented by the circles with radius  $t_c$ . The auxiliary data  $\text{AD}_2$  shifts the enrolment binary vector  $\mathbf{f}_B^e$  to the codeword  $\mathbf{C}$ . In the verification phase, the same shift is applied to  $\mathbf{f}_B^v$  and will lead to a match only if it is within the radius  $t_c$  of codeword  $\mathbf{C}$ . Hence, all binary vectors  $\mathbf{f}_B^v$  within the dashed circle with radius  $t_c$  and center point  $\mathbf{f}_B^e$  will lead to a match.

In this work we consider two cases of the FCS, namely the *unbalanced* and *balanced system*. For the unbalanced system there are  $N_e \neq N_v$  enrolment samples with  $N_v$  verification samples, while for the balanced case the number of verification samples is equal to the number of enrolment samples,  $N_v = N_e$ .

### C. Hamming Weight after XOR-ing two Random Binary Vectors

In many derivations in the remainder of this work we need a solution to the following problem. Consider the case of having two words  $\mathbf{w}_1$  and  $\mathbf{w}_2$  randomly selected from  $\{0, 1\}^{n_c}$  with weights  $w_1$  and  $w_2$ , respectively. Defining the number of bit errors or differences  $\epsilon$  between  $\mathbf{w}_1$  and  $\mathbf{w}_2$ , namely  $\epsilon = d_H(\mathbf{w}_1, \mathbf{w}_2)$ , we are interested in the probability mass function (pmf) of  $\epsilon$ .

**Lemma II.1** (Hamming Weight after the XOR of two Binary Vectors). *Given two random binary vectors  $\mathbf{w}_1$  and  $\mathbf{w}_2$  with Hamming weight  $w_1$  and  $w_2$ , respectively and defining  $w_{\min} = \min(w_1, w_2)$ , and  $w_{\max} = \max(w_1, w_2)$ , the number of possible bit errors  $\epsilon = d_H(\mathbf{w}_1, \mathbf{w}_2)$  is given by the set*

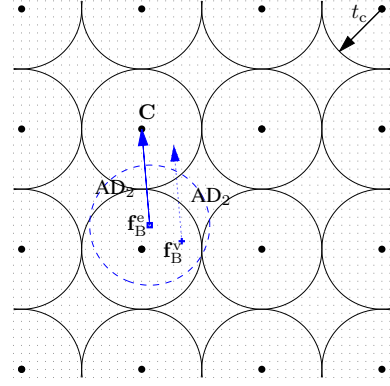


Fig. 2. An illustration of the FCS construction principles. The grid of small dots represent the word space  $\{0, 1\}^{n_c}$ , while the bigger dots represents the codewords from  $\mathcal{C}$  with the error-correcting capability represented by the circles with radius  $t_c$ .  $\text{AD}_2$  shifts the enrolment binary vector  $\mathbf{f}_B^e$  to the codeword  $\mathbf{C}$ . In the verification phase, the same shift is applied to  $\mathbf{f}_B^v$  and will lead to a match if it is within the radius  $t_c$  of codeword  $\mathbf{C}$ . Hence, all binary vectors  $\mathbf{f}_B^v$  within the dashed circle with radius  $t_c$  and center point  $\mathbf{f}_B^e$  will lead a match.

$E = \{\epsilon_{\min}, \epsilon_{\min} + 2, \dots, \epsilon_{\max} - 2, \epsilon_{\max}\}$  with probability  $P_{w \times w}(\epsilon; w_1, w_2, n_c)$  defined as

$$P_{w \times w}(\epsilon; w_1, w_2, n_c) \stackrel{\text{def}}{=} \begin{cases} 0 & \text{if } \epsilon \notin E \\ \frac{1}{\binom{n_c}{w_{\min}}} \binom{w_{\max}}{w_{\min} - (\epsilon - \epsilon_{\min})/2} \binom{n_c - w_{\max}}{(\epsilon - \epsilon_{\min})/2} & \text{if } \epsilon \in E \end{cases}, \quad (1)$$

where  $\epsilon_{\min} = |w_1 - w_2|$ , and  $\epsilon_{\max} = n_c - |w_1 + w_2 - n_c|$ .

*Proof:*

Because  $\mathbf{w}_1$  and  $\mathbf{w}_2$  have  $w_1$  and  $w_2$  bits of value 1, respectively, the minimum number of possible errors equals the difference  $\epsilon_{\min} = |w_1 - w_2|$ . For example, let  $w_1 > w_2$ , i.e.  $w_{\max} = w_1$  and  $w_{\min} = w_2$ , and the first  $w_1$  bits of  $\mathbf{w}_1$  have a value 1 while the remaining  $n_c - w_1$  bits have a value 0. The case with  $\epsilon_{\min}$  errors can be obtained by allocating the  $w_2$  bits of value 1 as the first bits of  $\mathbf{w}_2$ . Overall, there are  $\binom{w_1}{w_2}$  possible combinations of having  $w_2$  bits of value 1 of  $\mathbf{w}_2$  at locations where the bits of  $\mathbf{w}_1$  have a value of 1. Thus, the probability of having  $\epsilon_{\min}$  errors is equal to the ratio of the number of possibilities with respect to the number of binary vectors of length  $n_c$  with weight  $w_2$ , namely  $\binom{w_1}{w_2} / \binom{n_c}{w_2}$ .

Note that two bit errors are introduced if one bit of value 1 of  $\mathbf{w}_2$  is allocated where  $\mathbf{w}_1$  has a bit value of 0 instead of value 1. Hence, there are  $\binom{w_1}{w_2 - 1} \binom{n_c - w_1}{1}$  possible combinations of introducing 2 bit errors. The first binomial coefficient  $\binom{w_1}{w_2 - 1}$  is the number of possibilities of locating  $w_2 - 1$  bits of value 1 of  $\mathbf{w}_2$  at the  $w_1$  locations where  $\mathbf{w}_1$  has bits of value 1. The second binomial coefficient  $\binom{n_c - w_1}{1}$  is the number of possibilities of allocating a single bit of value 1 of  $\mathbf{w}_2$  at the  $n_c - 1$  locations where  $\mathbf{w}_1$  has a bit of value 0. Similarly, four bit errors are introduced when two bits of value 1 of  $\mathbf{w}_2$  are allocated where  $\mathbf{w}_1$  has a bit value of 0 with  $\binom{w_1}{w_2 - 2} \binom{n_c - w_1}{2}$  possible combinations.

The maximum number of bit errors  $\epsilon_{\max}$  is introduced by allocating all  $w_2$  bits of value 1 of  $\mathbf{w}_2$  at locations where the bits of  $\mathbf{w}_1$  have a value 0. When  $w_1 + w_2 > n_c$ , the number

of bits of  $w_1$  of value 0 is smaller than the number of bits of  $w_2$  of value 1, namely  $n_c - w_1 < w_2$ , because of the  $w_1 > w_2$  assumption. Consequently, the maximum number of bit errors is limited to  $\epsilon_{\max} = n_c - |w_1 + w_2 - n_c|$ . ■

### III. CROSS-MATCHING ATTACKS

The setup of the cross-matching analysis is depicted in Fig. 3. We consider the scenario where there are two applications using the same biometric trait and identical template protection algorithms. Each application creates a protected template from independent enrolment samples of its subjects and stores it into its centralized database. We consider both centralized databases to be accessible by the adversary. Furthermore, we consider two cases differing on what is stored in the centralized database. In the first case, Case 1, both the auxiliary data  $AD_2$  and the pseudonymous identifier  $PI$  are stored. Hence, the protected template for the first and second application is the pair  $\{PI_1, AD_{2,1}\}$  and  $\{PI_2, AD_{2,2}\}$ , respectively. In the second case, Case 2, we consider only  $AD_2$  to be stored in the centralized databases that are accessible, while  $PI$  may be stored within a personal storage device such as a smart-card which is not compromised. The adversary has access to all protected templates in both databases and tries to find subjects that are enrolled in both applications. Two protected templates, each taken from a different database, are compared by a *cross-matching classifier* in the *Comparator* module in order to determine whether they were derived from the same subject. The cross-matching classifier computes a cross-matching distance score  $s_{CM}$  on which to base its decision whether the two protected templates belong to the same subject (genuine) or not (imposter). The comparison between the protected templates of the same subject is referred to as a genuine comparison and between different subjects as an imposter comparison. The *false match rate* (FMR) at cross-matching  $\alpha_{CM}$  is the rate of claiming two templates to be from the same subjects at an imposter comparison. The *false non-match rate* (FNMR) at cross-matching  $\beta_{CM}$  is the rate of claiming two templates to be from different subjects at a genuine comparison. Ideally, these error rates should be as large as possible.

In this section, we discuss several cross-matching classifier methods. We discuss the exhaustive search approach for Case 1 and Case 2. We omitted the third possible case where only  $PI$  is stored in the centralized databases that are accessible by the adversary, because it can be easily shown that cross-matching is not possible. If the key could be derived from  $PI$ , they could still not be used for cross-matching because the keys were generated randomly within each application. Furthermore, we discuss the recently published method known as the decodability attack [14] [15], which is not based on an exhaustive search and only consists of an XOR and decoding operation by exploiting the linearity property of the ECC.

#### A. Exhaustive Search Attack

Given two protected templates, the exhaustive search type of the cross-matching attack relies on searching the complete codebook  $\mathcal{C}$  in order to determine whether the two protected

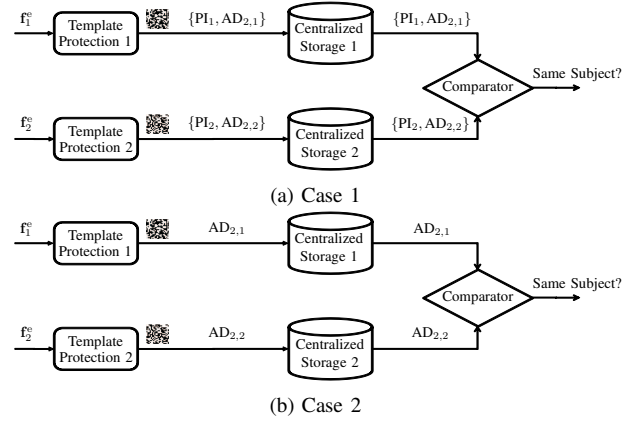


Fig. 3. Two cases of the cross-matching attack scenario between two application databases that are accessible by the adversary. The first case (Case 1) both  $PI$  and  $AD_2$  are stored in the centralized database. In the second case (Case 2) only  $AD_2$  is stored in the centralized database accessible by the adversary, while  $AD_2$  is assumed to be stored in a secure way and is not accessible by the adversary.

templates belong to the same subject.

**Case 1:  $PI$  and  $AD_2$ .** Recall that the pseudonymous identifier  $PI$  is the hash of the randomly selected key  $K$ . Because the  $PI$  is part of the protected template, a possible attack would be to search the key from the  $PI$ . Assuming that the probability of a collision is small, i.e. the probability that two different keys have the same hash value, the key leading to the hash value equal to  $PI$  can be found by searching the key space of  $\{0, 1\}^{k_c}$  and taking its hash value. The enrolled binary vector  $f_B^e$  can be obtained by computing the XOR of auxiliary data  $AD_2$  and the codeword  $C$  corresponding to the obtained key  $K$ , namely  $f_B^e = AD_2 \oplus C$ . By performing this exhaustive search on each protected template we obtain the binary vector  $f_{B,1}^e$  and  $f_{B,2}^e$  for the first and second application, respectively. As the cross-matching distance score  $s_{CM}$  we use the Hamming distance  $s_{CM} = \epsilon_{CM} = d_H(f_{B,1}^e, f_{B,2}^e)$ . On average only half of the key space has to be searched, hence the average effort of finding the key corresponding to  $PI$  is  $2^{k_c-1}$ . Consequently, finding both keys separately only takes twice the effort, namely  $2^{k_c}$ .

**Case 2: Only  $AD_2$ .** Because  $PI$  is not available, the distance measure has to be obtained from  $AD_2$  only. By defining the XOR operation of the two auxiliary data as  $AD_{\oplus} \stackrel{\text{def}}{=} AD_{2,1} \oplus AD_{2,2}$ , we can rewrite  $AD_{\oplus}$  as

$$\begin{aligned} AD_{\oplus} &= AD_{2,1} \oplus AD_{2,2} \\ &= (f_{B,1}^e \oplus C_1) \oplus (f_{B,2}^e \oplus C_2) \\ &= (f_{B,1}^e \oplus f_{B,2}^e) \oplus (C_1 \oplus C_2) \\ &= e \oplus C_3, \end{aligned} \quad (2)$$

where  $f_{B,1}^e$  ( $C_1$ ) and  $f_{B,2}^e$  ( $C_2$ ) are the binary vectors (codewords) in the enrolment phase for application 1 and 2 respectively,  $e$  is the error pattern between the enrolment binary vectors, and we used the property of linear codes where the XOR of two codewords leads to another codeword from the same codebook. A graphical representation of the XOR



decreases the FMR. Increasing the key size  $k_c$  and therefore decreasing the error-correcting capability  $t_c$ , also decreases the FMR.

As shown in Section III-B, the FMR of the cross-matching classifier  $\alpha_{CM}$  is the probability that the XOR of the auxiliary data from two different subjects is decodable. As defined in [15], under the assumption that the bits of  $\mathbf{f}_B$  are independent and uniform with  $P_e^{im} = \frac{1}{2}$ , the  $\alpha_{CM}$  is equal to the probability of randomly selecting a word  $\mathbf{w} \in_R \{0, 1\}^{n_c}$  that is decodable, i.e. within  $t_c$  bits of any codeword from  $\mathcal{C}$ , namely

$$\alpha_{CM}(t_c, n_c) \stackrel{\text{def}}{=} \mathcal{P}\{d_c(\mathbf{w}, \mathcal{C}) \leq t_c\} = \frac{2^{k_c} V_2(n_c, t_c)}{2^{n_c}}. \quad (5)$$

An illustration of the binary vectors that will lead to a match is shown in Fig. 5. The  $\alpha_{CM}(t_c, n_c)$  is equal to the ratio of all possible vectors within the dashed circles with respect to all possible vectors in the  $\{0, 1\}^n$  space. Examples of  $\alpha_{CM}(t_c, n_c)$  at some BCH ECC settings are given in Table II. Increasing the codeword size  $n_c$  decrease  $\alpha_{CM}(t_c, n_c)$ , however increasing the key size  $k_c$  does not always decrease  $\alpha_{CM}(t_c, n_c)$ . Note the special case of  $n_c = 31$  with  $[k_c, t_c] = [26, 1]$ , where  $\alpha_{CM} = 1$  because the full  $\{0, 1\}^{n_c}$  space is decodable. Thus, this  $[n_c, k_c, t_c]$  setting of the BCH ECC coincides with the Hamming code which is known to be perfect.

By combining the system FMR  $\alpha_{TP}$  from (4) and the cross-matching FMR  $\alpha_{CM}$  from (5) we obtain

$$\alpha_{CM}(t_c, n_c) = 2^{k_c} \alpha_{TP}(t_c, n_c), \quad (6)$$

which implies that the cross-matching FMR is  $2^{k_c}$  times larger than the system FMR under the assumption that the bits of  $\mathbf{f}_B^e$  across the population are independent and uniform. ■

### B. False Non-Match Rate Relationship

**Lemma IV.2** (FNMR Relationship). *Under the assumption that the bits of  $\mathbf{f}_B \in \{0, 1\}^{n_c}$  are independent with equal bit-error probability  $P_e^{ge}$ , given a balanced system where  $N_v = N_e$  and a  $t_c$ -error binary linear ECC, the cross-matching  $\beta_{CM}$  at the error correcting threshold  $t_c$  is smaller than the system FNMR  $\beta_{TP}$ , namely  $\beta_{CM}(t_c, n_c) < \beta_{TP}(t_c, n_c)$ .*

*Proof:* For the template protection system, a false non-match occurs when  $\epsilon = d_H(\mathbf{f}_B^e, \mathbf{f}_B^v) > t_c$  at genuine comparisons. Similar as in Section IV-A, we model the pmf of  $\epsilon$

TABLE II  
EXAMPLES OF  $\alpha_{TP}$  AND  $\alpha_{CM}$  FOR DIFFERENT  $n_c \in \{127, 63, 31\}$  AND  $[k_c, t_c]$  SETTINGS.

$n_c = 127$				
$[k_c, t_c]$	[8, 31]	[22, 23]	[36, 15]	[78, 7]
$\alpha_{TP}$	$3.16 \cdot 10^{-9}$	$8.48 \cdot 10^{-14}$	$7.89 \cdot 10^{-20}$	$5.57 \cdot 10^{-28}$
$\alpha_{CM}$	$8.10 \cdot 10^{-7}$	$3.56 \cdot 10^{-7}$	$5.42 \cdot 10^{-9}$	$1.68 \cdot 10^{-4}$
$n_c = 63$				
$[k_c, t_c]$	[7, 15]	[16, 11]	[24, 7]	[45, 3]
$\alpha_{TP}$	$1.88 \cdot 10^{-5}$	$8.37 \cdot 10^{-8}$	$6.82 \cdot 10^{-11}$	$4.52 \cdot 10^{-15}$
$\alpha_{CM}$	$2.41 \cdot 10^{-3}$	$5.48 \cdot 10^{-3}$	$1.14 \cdot 10^{-3}$	$1.59 \cdot 10^{-1}$
$n_c = 31$				
$[k_c, t_c]$	[6, 7]	[11, 5]	[16, 3]	[26, 1]
$\alpha_{TP}$	$1.66 \cdot 10^{-3}$	$9.61 \cdot 10^{-5}$	$2.32 \cdot 10^{-6}$	$1.49 \cdot 10^{-8}$
$\alpha_{CM}$	$1.06 \cdot 10^{-1}$	$1.97 \cdot 10^{-1}$	$1.52 \cdot 10^{-1}$	1.00

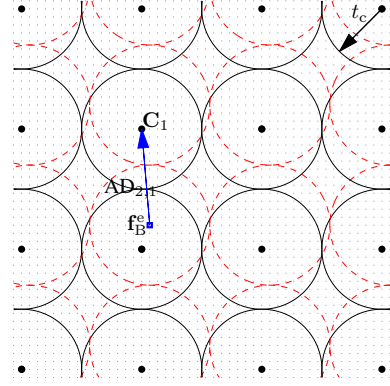


Fig. 5. An illustration of the binary vectors that would lead to a match.

with a binomial density with dimension  $n_c$ , however with bit-error probability  $P_e^{ge}$ . The theoretical FNMR of the template protection system at threshold  $t_c$ ,  $\beta_{TP}(t_c, n_c)$ , is the following sum of the binomial pmf

$$\beta_{TP}(t_c, n_c) \stackrel{\text{def}}{=} \sum_{i=t_c+1}^{n_c} P_b(i; n_c, P_e^{ge}). \quad (7)$$

For the cross-matching classifier,  $\beta_{CM}$  is the probability that the XOR of the auxiliary data  $AD_{2,1}$  and  $AD_{2,2}$  from the same subject at different databases is not decodable, hence an non-match at a genuine comparison. As discussed in Section III-A, the decodability probability is determined by the Hamming distance between the binary vectors at enrolment, namely  $\epsilon_{CM} = d_H(\mathbf{f}_{B,1}^e, \mathbf{f}_{B,2}^e)$ . Because of the balanced system assumption the bit-error probability is also equal  $P_e^{ge}$ , consequently the pmf of  $\epsilon_{CM} = d_H(\mathbf{f}_{B,1}^e, \mathbf{f}_{B,2}^e)$  is equal to the pmf of  $\epsilon = d_H(\mathbf{f}_B^e, \mathbf{f}_B^v)$  and for convenience we use  $\epsilon$  in the remainder of this section. As discussed in Section III, there is also a probability that when  $\epsilon > t_c$ , the XOR of the auxiliary data  $AD_{\oplus}$  will also be decodable and hence correctly labeled as genuine. We define the decodability probability  $P_{AD_{\oplus}}(\epsilon; t_c, \mathcal{C})$  as

$$P_{AD_{\oplus}}(\epsilon; t_c, \mathcal{C}) \stackrel{\text{def}}{=} \mathcal{P}\{d_c(AD_{\oplus}, \mathcal{C}) \leq t_c \mid \epsilon\} \quad (8)$$

which has to be taken into account when estimating  $\beta_{CM}$  according to

$$\beta_{CM}(t_c, n_c) \stackrel{\text{def}}{=} \sum_{i=t_c+1}^{n_c} \left(1 - P_{AD_{\oplus}}(i; t_c, \mathcal{C})\right) P_b(i; n_c, P_e^{ge}). \quad (9)$$

Observe that  $\beta_{CM}(t_c, n_c)$  from (9) is equal to  $\beta_{TP}(t_c, n_c)$  from (7) when  $\left(1 - P_{AD_{\oplus}}(\epsilon; t_c, \mathcal{C})\right) = 1$  for  $\epsilon > t_c$ . In other words  $P_{AD_{\oplus}}(\epsilon; t_c, \mathcal{C}) = 0$  stating that  $AD_{\oplus}$  should not be decodable for any cases of  $\mathbf{f}_B^e$  and  $\mathbf{f}_B^v$  with error pattern of weight  $\epsilon > t_c$ . However,  $\beta_{CM}(t_c, n_c) < \beta_{TP}(t_c, n_c)$  if there is at least one case of  $\mathbf{f}_B^e$  and  $\mathbf{f}_B^v$  with error pattern of weight  $\epsilon > t_c$  where  $AD_{\oplus}$  is decodable. Hence, it suffice to prove that there is at least one case of  $\mathbf{f}_B^e$  and  $\mathbf{f}_B^v$  with error pattern of weight  $\epsilon > t_c$  where  $AD_{\oplus}$  is decodable.

Let the codebook be  $\mathcal{C} = \{C_1, C_2, C_3\}$  with minimum distance  $d = 2t_c + 1$ , where the codewords  $C_1$  and  $C_2$  are used in the enrolment phase of application 1 and 2, respectively, and

$\mathbf{C}_3 = \mathbf{C}_1 \oplus \mathbf{C}_2$ . Note that the XOR of the auxiliary data can be rewritten as  $\text{AD}_\oplus = (\mathbf{f}_{\text{B},1}^e \oplus \mathbf{C}_1) \oplus (\mathbf{f}_{\text{B},2}^e \oplus \mathbf{C}_2) = \mathbf{e} \oplus \mathbf{C}_3$  with  $\epsilon = \|\mathbf{e}\|$  and is decodable for the  $\epsilon > t_c$  cases only if the error pattern can be rewritten as  $\mathbf{e} = \mathbf{e}^* \oplus \mathbf{C}_i$  with  $\|\mathbf{e}^*\| \leq t_c$  and  $\mathbf{C}_i \in \{\mathbf{C}_1, \mathbf{C}_2\}$ . Hence, there are at least two cases where  $\text{AD}_\oplus$  with  $\epsilon > t_c$  is decodable, namely the cases  $\text{AD}_\oplus = \mathbf{C}_1 \oplus \mathbf{C}_3$  or  $\text{AD}_\oplus = \mathbf{C}_2 \oplus \mathbf{C}_3$  where  $\|\mathbf{e}^*\| = 0$ . ■

Lemma IV.2 only states that  $\beta_{\text{CM}}(t_c, n_c) < \beta_{\text{TP}}(t_c, n_c)$  for any settings of  $t_c$  and  $n_c$ . In order to know the actual difference between  $\beta_{\text{CM}}(t_c, n_c)$  and  $\beta_{\text{TP}}(t_c, n_c)$  we have to determine  $P_{\text{AD}_\oplus}(\epsilon; t_c, \mathcal{C})$  given a specific codebook  $\mathcal{C}$ . Assume we have an ECC with the codebook  $\mathcal{C}$  consisting of one codeword of weight 0 ( $\mathbf{C}_0$ ) and  $n_c$  ( $\mathbf{C}_{n_c}$ ) and  $n_w$  codewords  $\mathbf{C}_w$  of weight  $w$ . Because of the properties of linear codes, each codeword has  $n_w$  neighbors at a distance  $w$  and one codeword at a distance  $n_c$ . Consider the case of being at codeword  $\mathbf{C}_0$  and having a binary vector  $\mathbf{w}_\epsilon$  with  $\epsilon$  errors with respect to  $\mathbf{C}_0$ , hence having the weight  $w_\epsilon$ . There are  $n_w$  neighboring codewords at a distance of  $w$  bits from  $\mathbf{C}_0$ , thus they have a weight of  $w$ . Furthermore, the error-correcting capability is equal to  $t_c$ . The fundamental question we want to answer is the decodability probability of the binary vector of  $\mathbf{w}_\epsilon$ . If its weight  $w_\epsilon$  is within the error-correcting capability  $t_c$ ,  $w_\epsilon \leq t_c$ ,  $\mathbf{w}_\epsilon$  will always be decodable with respect to  $\mathbf{C}_0$ . However, if  $w_\epsilon > t_c$  the binary vector  $\mathbf{w}_\epsilon$  will not be decodable with respect to  $\mathbf{C}_0$  but there is a probability that  $\mathbf{w}_\epsilon$  is decodable with respect to one of the  $n_w$  neighboring codewords at distance  $w$ .  $\mathbf{w}_\epsilon$  will only be decodable if its distance to the neighboring codewords is smaller or equal to  $t_c$ , i.e.  $\|\mathbf{w}_\epsilon \oplus \mathbf{C}_w\| \leq t_c$ . In Section II-C we have discussed the probability  $P_{w \times w}(\epsilon; w_1, w_2, n_c)$  of the weight of the binary vector after XOR-ing two binary vectors of length  $n_c$  and weights  $w_1$  and  $w_2$ , respectively. Hence, the decodability probability with respect to the  $n_w$  neighboring codewords of weight  $w$  is equal to  $n_w \sum_{i=0}^{t_c} P_{w \times w}(i; w_\epsilon, w, n_c)$ . Similarly, the decodability probability with respect to the codeword  $\mathbf{C}_{n_c}$  has to be included, which is equal to  $\sum_{i=0}^{t_c} P_{w \times w}(i; w_\epsilon, n_c, n_c)$ .

For a general codebook  $\mathcal{C}$ , the decodability probability at  $\epsilon$  errors,  $P_{\text{AD}_\oplus}(\epsilon; t_c, \mathcal{C})$ , is given by

$$P_{\text{AD}_\oplus}(\epsilon; t_c, \mathcal{C}) = \sum_{w \in W_{\mathcal{C}}} N_{\mathcal{C}}(w) \sum_{i=0}^{t_c} P_{w \times w}(i; \epsilon, w, n_c), \quad (10)$$

where  $W_{\mathcal{C}}$  is the set of the unique weights  $w$  of the codewords from  $\mathcal{C}$  and the function  $N_{\mathcal{C}}(w)$  returns the number of codewords  $n_w$  with weight  $w$ , with  $\sum_{w \in W_{\mathcal{C}}} N_{\mathcal{C}}(w) = |\mathcal{C}|$ . Some

examples of  $P_{\text{AD}_\oplus}(\epsilon; t_c, \mathcal{C})$  for the BCH code we consider are portrayed in Fig. 6 for  $n_c \in \{31, 63\}$  and different  $t_c$  settings. From these figures we can conclude that when  $\epsilon \geq n_c - t_c$ ,  $\text{AD}_\oplus$  will always be decodable, because of the existence of a complementary codeword at distance  $n_c$  with respect to each codeword from  $\mathcal{C}$ . Furthermore, when  $n_c = 31$  at most  $\approx 20\%$  of the cases where  $t_c < \epsilon < n_c - t_c$  are still decodable, which is significantly decreased to  $\approx 0.6\%$  when  $n_c = 63$ . Some examples of  $\beta_{\text{TP}}$  and  $\beta_{\text{CM}}$  for different  $n_c \in \{31, 63\}$  and  $P_e^{\text{ge}} \in \{0.20, 0.15\}$  settings are given in Table III. There is no

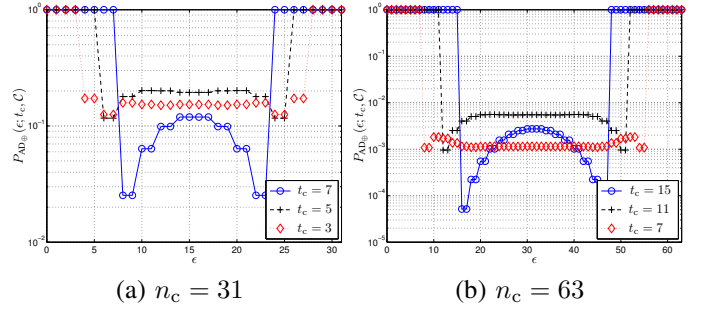


Fig. 6.  $P_{\text{AD}_\oplus}(\epsilon; t_c, \mathcal{C})$  values for different  $t_c$  settings at  $n_c \in \{31, 63\}$ .

significant difference between  $\beta_{\text{TP}}$  and  $\beta_{\text{CM}}$  for the  $n_c = 63$  case, however there is a clear difference for the  $n_c = 31$  case.

### C. Performance Relationship

**Conjecture IV.1** (Performance Relationship). *Under the assumption that the bits of  $\mathbf{f}_{\text{B}} \in \{0,1\}^{n_c}$  are independent with equal bit-error probability  $P_e^{\text{ge}}$  and  $P_e^{\text{im}} = \frac{1}{2}$  at genuine and imposter comparisons respectively, given a balanced system where  $N_v = N_e$  the cross-matching performance is worse than the system performance.*

With Lemma IV.1 we showed that FMR between the cross-matching and system is related according to  $\alpha_{\text{CM}}(t_c, n_c) = 2^{k_c} \alpha_{\text{TP}}(t_c, n_c)$ , where the cross-matching FMR is  $2^{k_c}$  worse than the system FMR. However, with Lemma IV.2 we showed that the FNMR at cross-matching is better than the system FNMR, however the difference is marginal at larger codeword lengths. In order to compare the overall performance we use the *receiver operating characteristic* (ROC) curves as illustrated in Fig. 7 for the  $n_c \in \{31, 63\}$  and  $P_e^{\text{ge}} = 0.15$  settings. The system performance is given by the ROC labeled as  $\text{TP}_b$ , while the cross-matching performance is indicated by the points labeled with different markers representing the different  $[k_c, t_c]$  settings of the ECC. Note that a performance is considered as being better when it is closer to the upper-left corner of the graph. Because the system ROC curve is clearly closer to the upper-left corner, we have shown that the system performance is better than the cross-matching performance.

TABLE III  
COMPARISON BETWEEN  $\beta_{\text{TP}}$  AND  $\beta_{\text{CM}}$  FOR DIFFERENT  $n_c \in \{31, 63\}$ ,  $[k_c, t_c]$  AND  $P_e^{\text{ge}} \in \{0.15, 0.20\}$  SETTINGS.

$n_c = 31$				
$[k_c, t_c]$		[6, 7]	[11, 5]	[16, 3]
$P_e^{\text{ge}} = 0.15$	$\beta_{\text{TP}}$	0.0822	0.3173	0.7039
	$\beta_{\text{CM}}$	0.0796	0.2749	0.5948
$P_e^{\text{ge}} = 0.20$	$\beta_{\text{TP}}$	0.2700	0.6069	0.8930
	$\beta_{\text{CM}}$	0.2598	0.5176	0.7592
$n_c = 63$				
$[k_c, t_c]$		[7, 15]	[16, 11]	[24, 7]
$P_e^{\text{ge}} = 0.15$	$\beta_{\text{TP}}$	0.0215	0.2287	0.7471
	$\beta_{\text{CM}}$	0.0215	0.2283	0.7460
$P_e^{\text{ge}} = 0.20$	$\beta_{\text{TP}}$	0.1789	0.6246	0.9527
	$\beta_{\text{CM}}$	0.1789	0.6231	0.9513

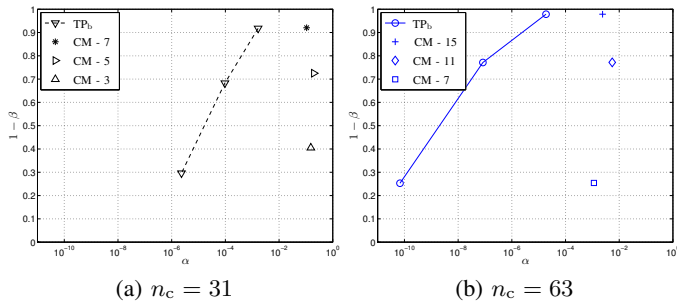


Fig. 7. Performance comparison between the template protection system (TP<sub>b</sub>) and cross-matching performance (CM) for the (a)  $n_c = 31$  and (b)  $n_c = 63$  case, under the assumption of independent bits with bit-error probabilities  $P_e^{\text{im}} = 0.5$  and  $P_e^{\text{ge}} = 0.15$ , and a balanced system  $N_e = N_v$ . The suffix indicates  $t_c$ .

## V. EXPERIMENTS

In this section we empirically estimate both the template protection system and cross-matching performance based on a fingerprint database in Section V-B and Section V-C, respectively. The biometric database, feature extraction and evaluation protocol are described in Section V-A.

### A. Experimental Setup

1) *Biometric Modality and Database*: The database we use is the MCYT (Ministerio de Ciencia y Tecnología) containing fingerprint images from a capacitive and optical sensor as described in [19]. It contains 12 images of all 10 fingers from  $N_s = 330$  subjects for each sensor. However, we limit our dataset to the images of the right-index finger from the optical sensor.

2) *Feature Extraction Algorithms*: In order to compensate for possible translations between the enrolment and verification measurements, a translation-only pre-alignment step is performed during the feature extraction process. Such pre-alignment requires extraction of the core point which is performed according to the algorithm described in [20]. Around the core point we define a  $17 \times 17$  grid with eight pixels between each grid point. The feature extraction algorithm extracts a feature value on each grid point. Our feature extraction algorithm failed to extract a feature vector from a single subject, so we excluded it from the dataset, hence there are effectively  $N_s = 329$  subjects.

The feature extraction method is based on the Gabor filter response, described in [21], where each grid point is filtered using a set of four 2D Gabor filters at angles of  $\{0, \frac{\pi}{4}, \frac{\pi}{2}, \frac{3\pi}{4}\}$ , respectively. The feature vector is the concatenation of the modulus of the four complex responses at each grid point, resulting into a feature vector dimension of  $N_F = 1156$ .

3) *Performance Evaluation Protocol*: The performance evaluation protocol consists of randomly selecting 219 out of  $N_s = 329$  subjects as the training set and the remaining 110 subjects as the evaluation set, which is referred to as the training-evaluation-set split. To decorrelate the feature components we use the principle component analysis (PCA) and the linear discriminant analysis (LDA) techniques. The PCA and LDA transformation matrices are computed using

the training set, where  $N_{\text{PCA}}$  is the reduced dimension after applying the PCA transformation and  $N_{\text{LDA}}$  is the reduced dimension after applying the LDA transformation. Furthermore, the template protection system parameters such as the quantization thresholds, used within the *Bit Extraction* module, are also estimated on the training set.

From the evaluation set we evaluate both the system and cross-matching classification performance.

- For the *system performance* evaluation,  $N_e$  samples of each subject are randomly selected as the enrolment samples while the remaining samples are considered as the verification samples. The protected template is generated using all the  $N_e$  enrolment samples and compared with disjoint groups of  $N_v$  verification samples where the mean of the feature vectors is taken prior to the bit extraction process.
- For the *cross-matching performance* evaluation, we randomly select  $N_e$  samples for the enrolment for the first application and another random  $N_e$  samples for the second application as such that we have distinct samples for each application. For each application we create the protected template and compare all protected templates using the cross-matching classifier.

This split of creating the enrolment and verification set or the enrolment set for application one and two is referred to as the enrolment-verification split. If the verification sample is from the same subject as of the protected template, it is referred to as a genuine comparison, otherwise it is an imposter comparison.

Both the training-evaluation-set and the enrolment-verification splits are performed five times. Note that the splits are performed randomly, however the seed at the start of the protocol is always the same, hence all the splits are equal for the performance tests at different settings. Therefore, the splitting process does not contribute to any performance differences.

### B. Template Protection System Performance

We evaluate the template protection system classification performance using the evaluation protocol in Section V-A3 with  $N_e = 6$  and  $N_v \in \{1, 6\}$ . The case where  $N_v = N_e$  is referred to as the balanced (TP<sub>b</sub>) case and the unbalanced (TP<sub>u</sub>) case when  $N_v \neq N_e$ .

The optimal  $N_{\text{PCA}}$  setting was found to be around 220 components and we set  $N_{\text{LDA}}$  equal to  $n_c$  to evaluate the performance. Note that we assume the FCS construction to act as a Hamming distance classifier as discussed in Section II, hence we actually evaluate the scores  $s_{\text{TP}} = \epsilon = d_{\text{H}}(\mathbf{f}_{\text{B}}^e, \mathbf{f}_{\text{B}}^v)$  and limit the ROC curve at the threshold equal to  $t_c$ . The ROC curves for  $n_c \in \{31, 63\}$  settings are portrayed in Fig. 8. The ROC curves are obtained by varying the  $k_c$  and  $t_c$  settings. For both  $n_c$  settings, the balanced case has a better performance because taking the average of  $N_v$  feature vectors suppresses the noise during verification which significantly improves the performance. Because of the BCH error-correcting limitation the FNMR is lower bounded and the FMR is upper bounded. The performance of the  $n_c = 63$  case is better, however the BCH limitation has a greater impact on the FNMR and FMR.

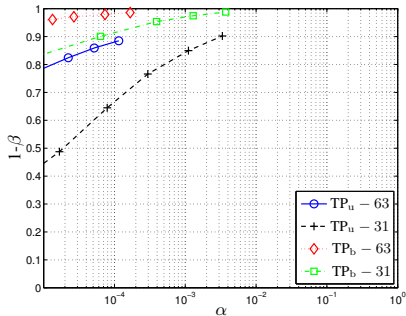


Fig. 8. The ROC curve of the balanced and unbalanced and (TP<sub>u</sub>) template protection system derived from the  $s_{\text{TP}} = d_{\text{H}}(\mathbf{f}_{\text{B}}^{\text{e}}, \mathbf{f}_{\text{B}}^{\text{v}})$  scores for the  $n_c \in \{31, 63\}$  settings. For the balanced case we have  $N_e = N_v = 6$ , while  $N_e = 6$  and  $N_v = 1$  for the unbalanced case.

Note that the experimentally obtained  $\alpha_{\text{TP}}$ , given in Table IV, for both the balanced and unbalanced case are very similar, however they deviate from the theoretical expectation presented in Section IV. Comparing Table II and Table IV, the experimentally obtained  $\alpha_{\text{TP}}$  at  $t_c$  is roughly an order of magnitude larger for the  $n_c = 63$  case, while twice larger for the  $n_c = 31$  case. We conjecture that the main cause of the deviating is the fact that the bits are still slightly dependent, while the theoretic work assumed independent bits. We omitted the  $n_c = 127$  case due to the limited dataset with respect to its small theoretic FMR at the maximum error-correcting capability  $t_c^*$ , namely  $\alpha_{\text{TP}}(t_c^* = 31, n_c = 127) \approx 3.16 \cdot 10^{-9}$ .

### C. Cross-Matching Performance Evaluation

As discussed in Section V-A3 for the cross-matching (CM) performance evaluation we create two datasets containing the same subjects with  $N_e = 6$  distinct samples of each subject. The two datasets represent the enrolment samples for the two applications. From the each dataset we compute the binary vectors  $\mathbf{f}_{\text{B},1}^{\text{e}}$  and  $\mathbf{f}_{\text{B},2}^{\text{e}}$ , and auxiliary data  $\text{AD}_{2,1}$  and  $\text{AD}_{2,2}$  from two randomly generated codewords  $\mathbf{C}_1$  and  $\mathbf{C}_2$ , respectively.

The cross-matching classifier from the decodability attack, as presented in Section III-B, is based on the property whether the XOR of the auxiliary data  $\text{AD}_{\oplus} = \text{AD}_{2,1} \oplus \text{AD}_{2,2}$  is decodable, i.e.  $\text{Dec}(\text{AD}_{\oplus})$  is successful, where  $\text{Dec}$  is the ECC decoding function. When successful the classifier outputs a match, otherwise a non-match. The decoding function of the BCH ECC we use does not return an error when it is not decodable, but returns the first  $k_c$  bits of  $\text{AD}_{\oplus}$  as the key instead. Therefore, we compute the cross-matching distance score  $s_{\text{CM}}$  as

$$s_{\text{CM}} = \begin{aligned} & d_{\text{CM}}(\text{AD}_{2,1}, \text{AD}_{2,2}) \\ & = d_{\text{H}}(\text{AD}_{\oplus}, \text{Enc}(\text{Dec}(\text{AD}_{\oplus}))), \end{aligned} \quad (11)$$

where  $d_{\text{CM}}$  is the distance measure of the cross-matching classifier, and  $\text{Enc}$  and  $\text{Dec}$  are the encoding and decoding function of the BCH ECC, respectively. Consequently, we can extend the cross-matching classifier beyond the decision of either match or non-match with a score indicating how similar the comparison is.

The cross-matching performance ROC curves (CM) are depicted in Fig. 9 for  $n_c = \{31, 63\}$  and different  $[k_c, t_c]$

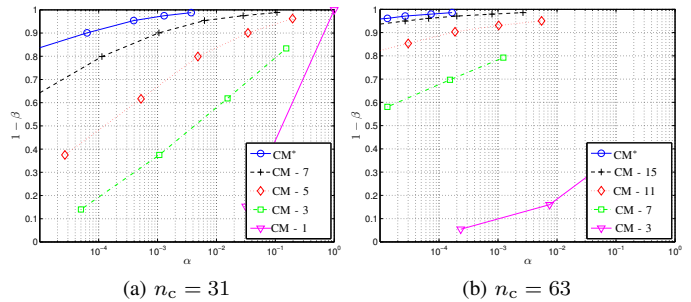


Fig. 9. The ROC curve of cross-matching using  $\text{AD}_2$  (CM) at different  $n_c$  and  $t_c$  indicated by the suffix. As reference, the ROC curve corresponding to  $\epsilon_{\text{CM}} = d_{\text{H}}(\mathbf{f}_{\text{B},1}^{\text{e}}, \mathbf{f}_{\text{B},2}^{\text{e}})$  is used and is labeled as CM\*.

settings. Because of the availability of a score value instead of a decision, the ROC curves consist of multiple points instead of a single point as in Fig. 7, where the outmost right-upper point corresponds to the decision-based performance. The  $\alpha_{\text{CM}}$  and  $\beta_{\text{CM}}$  values of these points are provided in Table IV. We also show the ROC curve from the Hamming distance of the enrolled binary vectors,  $\epsilon_{\text{CM}} = d_{\text{H}}(\mathbf{f}_{\text{B},1}^{\text{e}}, \mathbf{f}_{\text{B},2}^{\text{e}})$ , indicated by CM\*. Note that the CM\* ROC curve is equal to the balanced system performance ROC curve TP<sub>b</sub> from Fig. 8. Thus confirming the assumption made in Section IV-B that the pmf of  $\epsilon = d_{\text{H}}(\mathbf{f}_{\text{B}}^{\text{e}}, \mathbf{f}_{\text{B}}^{\text{v}})$  is equal to the pmf of  $\epsilon_{\text{CM}} = d_{\text{H}}(\mathbf{f}_{\text{B},1}^{\text{e}}, \mathbf{f}_{\text{B},2}^{\text{e}})$ . Note that when comparing Table II and Table IV, the experimentally obtained  $\alpha_{\text{CM}}$  are close to their theoretical expectation. Also note that we do not observe the same order of estimation errors as for the case of the system performance  $\alpha_{\text{TP}}$ .

With Fig. 9 we also experimentally validate Lemma IV.1 dictating that the cross-matching performance is always worse than the balanced system performance. Also note that the difference significantly increases when  $t_c$  is decreased and thus increasing  $k_c$ . However, the cross-matching performance can be better than the unbalanced system performance as shown by the comparison of the TP<sub>u</sub> - 31 and TP<sub>u</sub> - 63 ROC curves from Fig. 8 with the CM-7 and CM-15 curves from Fig. 9(a) and Fig. 9(b), respectively. Hence, designing a balanced system with  $N_e = N_v$  guarantees that the cross-matching performance is always worse than the system performance itself.

Comparing Table II and Table IV,

For further analysis we show the comparison between the cross-matching Hamming distance  $\epsilon_{\text{CM}}$  and distance score  $s_{\text{CM}}$  in Fig. 10. Note that the attacker only knows  $s_{\text{CM}}$  but not  $\epsilon_{\text{CM}}$ . These figures illustrate that for both the genuine and imposter comparisons if  $\epsilon_{\text{CM}} \leq t_c$  than  $s_{\text{CM}} \leq t_c$ . Furthermore, from the imposter comparisons, notably for the  $n_c = 31$  case, we also observe that when  $\epsilon_{\text{CM}} \geq n_c - t_c$  than it holds that  $s_{\text{CM}} = n_c - \epsilon_{\text{CM}}$ , because for each codeword there also exists its complementary one with a distance of  $n_c$  bits. For the case when  $t_c < \epsilon < n_c - t_c$ ,  $\text{AD}_{\oplus}$  is occasionally decodable leading to a score  $s_{\text{CM}} \leq t_c$  with probability  $P_{\text{AD}_{\oplus}}(\epsilon; t_c, \mathcal{C})$  from (10) only when we can rewrite  $(\mathbf{f}_{\text{B},1}^{\text{e}} \oplus \mathbf{f}_{\text{B},2}^{\text{e}}) = \mathbf{C}_i \oplus \mathbf{e}^*$  with  $\|\mathbf{e}^*\| \leq t_c$  and  $\mathbf{C}_i \in \mathcal{C}$ .

Also note that the average of the scores  $s_{\text{CM}}$ , for the

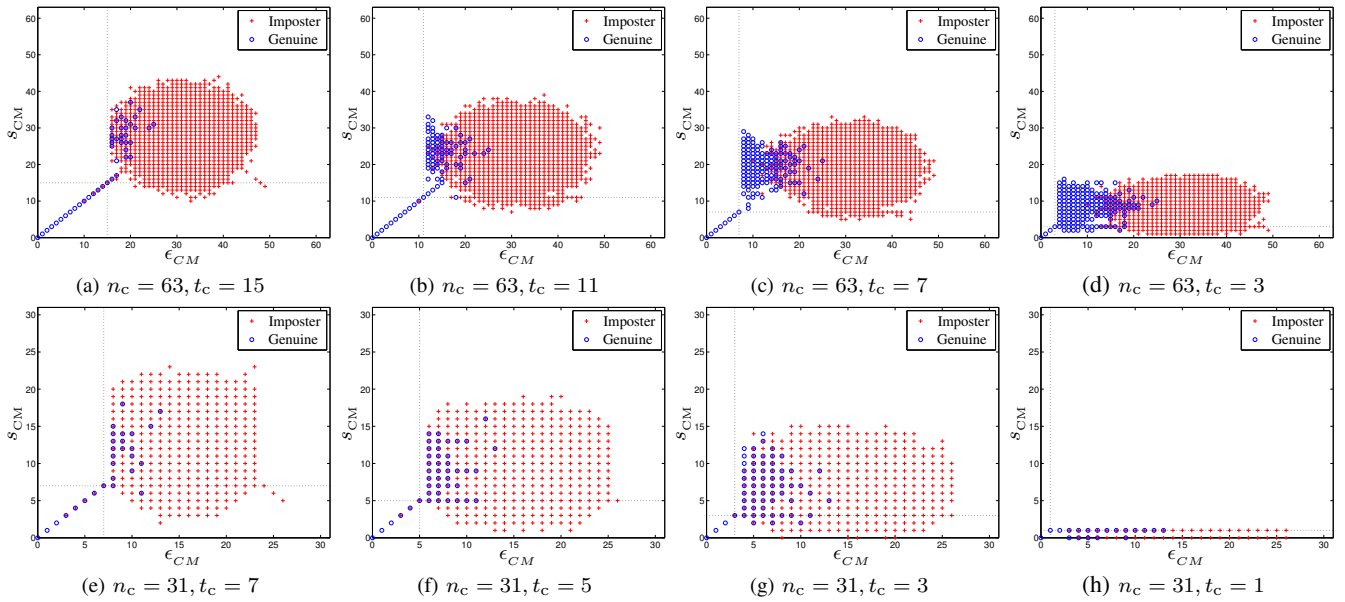


Fig. 10. Comparison between  $\epsilon_{CM} = d_H(\mathbf{f}_{B,1}^e, \mathbf{f}_{B,2}^e)$  and  $s_{CM} = d_{CM}(AD_{2,1}, AD_{2,2})$  for  $n_c = \{31, 63\}$  and different  $[k_c, t_c]$  settings.

cases when  $AD_{\oplus}$  is not decodable and leading to a score  $s_{CM} > t_c$ , decreases when  $t_c$  decreases. Because of the systematic implementation of the BCH ECC and the fact that the decoding function of the ECC returns the first  $k_c$  bits as the key, guarantees that the first  $k_c$  bits between the corresponding codeword and  $AD_{\oplus}$  are always equal while the remaining bits will be random. Hence, the expected bit difference is equal to  $\frac{n_c - k_c}{2}$ .

## VI. DECODABILITY ATTACK RESILIENCE WITH BIT-PERMUTATION RANDOMIZATION

We have shown that cross-matching is possible by using the decodability attack. However, if the system is designed as such that it is balanced, namely  $N_e = N_v$ , the cross-matching performance is always worse than the system performance, but still having a discriminating power. Ideally, it is preferred that the cross-matching performance is as close as possible to random.

In this section we introduce a randomization module within

TABLE IV  
EXPERIMENTALLY OBTAINED SYSTEM PERFORMANCE ( $\alpha_{TP}, \beta_{TP}$ ) AND CROSS-MATCHING PERFORMANCE ( $\alpha_{CM}, \beta_{CM}$ ) FOR DIFFERENT  $n_c \in \{31, 63\}$  AND  $[k_c, t_c]$  SETTINGS.

$n_c = 63$				
$[k_c, t_c]$	[7, 15]	[16, 11]	[24, 7]	[45, 3]
$\alpha_{TP}$	$1.67 \cdot 10^{-4}$	$3.34 \cdot 10^{-6}$	$\approx 0$	$\approx 0$
$\alpha_{CM}$	$2.64 \cdot 10^{-3}$	$5.47 \cdot 10^{-3}$	$1.23 \cdot 10^{-3}$	$1.58 \cdot 10^{-1}$
$\beta_{TP}$	$1.41 \cdot 10^{-2}$	$5.02 \cdot 10^{-2}$	$2.08 \cdot 10^{-1}$	$7.12 \cdot 10^{-1}$
$\beta_{CM}$	$1.42 \cdot 10^{-2}$	$4.98 \cdot 10^{-2}$	$2.08 \cdot 10^{-1}$	$5.89 \cdot 10^{-1}$
$n_c = 31$				
$[k_c, t_c]$	[6, 7]	[11, 5]	[16, 3]	[26, 1]
$\alpha_{TP}$	$3.72 \cdot 10^{-3}$	$3.94 \cdot 10^{-4}$	$3.34 \cdot 10^{-6}$	$\approx 0$
$\alpha_{CM}$	$1.07 \cdot 10^{-1}$	$1.96 \cdot 10^{-1}$	$1.53 \cdot 10^{-1}$	1.00
$\beta_{TP}$	$1.20 \cdot 10^{-2}$	$4.62 \cdot 10^{-2}$	$2.01 \cdot 10^{-1}$	$6.25 \cdot 10^{-1}$
$\beta_{CM}$	$1.13 \cdot 10^{-2}$	$3.78 \cdot 10^{-2}$	$1.66 \cdot 10^{-1}$	0

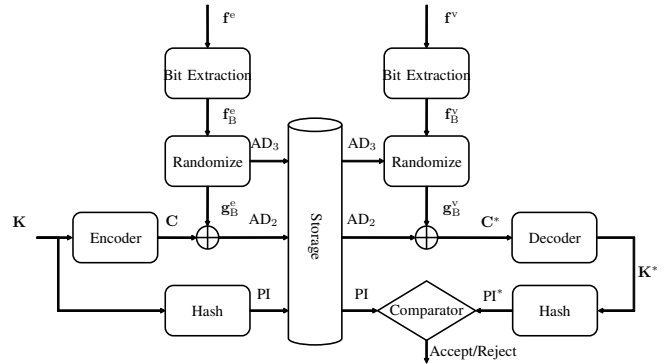


Fig. 11. The code-offset system with randomization.

the FCS construction rendering the cross-matching performance close to random. As illustrated in Fig. 11, prior to the XOR operation of the binary vector  $\mathbf{f}_B^e$  and the codeword, we randomize  $\mathbf{f}_B^e$  by multiplying it with a bit-permutation matrix  $A_\pi \in \Pi$ , obtaining  $\mathbf{g}_B^e = A_\pi \mathbf{f}_B^e$ , where  $A_\pi$  is a  $n_c \times n_c$  matrix derived by randomly permuting the rows of the identity matrix and  $\Pi$  is the set of all possible permutation matrices. Because  $A_\pi$  is an orthogonal matrix its inverse is equal to its transpose,  $A_\pi^{-1} = A_\pi'$ . At each enrolment a new randomly generated bit-permutation matrix is used and stored as auxiliary data  $AD_3$  and is considered as public. It is important to note that in the current approach the randomization matrix  $A_\pi$  is not considered to be secret, which is in contrast to earlier methods such as [13].

The XOR of the auxiliary data  $AD_{\oplus}$  can now be rewritten as

$$\begin{aligned}
 AD_{\oplus} &= (\mathbf{g}_{B,1}^e \oplus \mathbf{C}_1) \oplus (\mathbf{g}_{B,2}^e \oplus \mathbf{C}_2) \\
 &= (A_{\pi,1} \mathbf{f}_{B,1}^e \oplus A_{\pi,2} \mathbf{f}_{B,2}^e) \oplus (\mathbf{C}_1 \oplus \mathbf{C}_2) \\
 &= \mathbf{e}_\pi \oplus \mathbf{C}_3,
 \end{aligned} \tag{12}$$

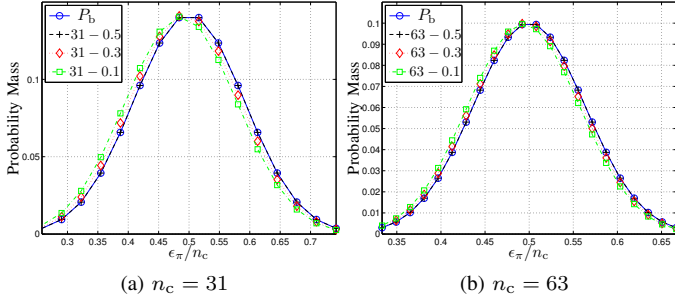


Fig. 12. The pmf of  $\epsilon_\pi = d_H(\mathbf{g}_{B,1}^e, \mathbf{g}_{B,2}^e)$  from (13) at genuine comparisons for settings of  $P_e^{\text{ge}} \in \{\frac{1}{10}, \frac{3}{10}, \frac{1}{2}\}$  and  $n_c = \{31, 63\}$  compared with a binomial distribution  $P_b(\epsilon_\pi; n_c, \frac{1}{2})$ .

with  $\epsilon_\pi = \|\mathbf{e}_\pi\| = d_H(A_{\pi,1}\mathbf{f}_{B,1}^e, A_{\pi,2}\mathbf{f}_{B,2}^e) = d_H(\mathbf{g}_{B,1}^e, \mathbf{g}_{B,2}^e)$  being the number of errors after permutation instead of  $\epsilon_{CM} = d_H(\mathbf{f}_{B,1}^e, \mathbf{f}_{B,2}^e)$  when no permutation has been applied. Because of the randomization process it is likely that at genuine comparisons more errors are introduced, namely  $\epsilon_\pi > \epsilon_{CM}$ , hence decreasing the probability that  $\text{AD}_\oplus$  is decodable, which significantly decreases when  $\epsilon_\pi > t_c$  (see Fig. 6). As discussed in Section III, under the assumption of having independent bits with bit-error probability  $P_e^{\text{ge}}$  between genuine comparisons, the pmf of  $\epsilon_\pi$  can be modeled by a binomial distribution with dimension  $n_c$  and  $p = P_e^{\text{ge}}$ , namely  $P_b(\epsilon_{CM}; n_c, P_e^{\text{ge}})$ . However, the pmf of  $\epsilon_\pi$  will depend on both the pmf of  $\epsilon_\pi$  and on the effect of the permutation, which we will analyze further. When the weight of the binary vectors  $\mathbf{f}_{B,1}^e$  and  $\mathbf{f}_{B,2}^e$  are  $w_1$  and  $w_2$ , respectively, the probability of  $\epsilon_\pi$  number of errors after randomizing them is thus equal to  $P_{w \times w}(\epsilon_\pi; w_1, w_2, n_c)$  as discussed in Section II-C. Hence, the expected probability of  $\epsilon_\pi$  irrespective of the weights  $P_{\epsilon_\pi}(\epsilon_\pi; P_e^{\text{ge}}, n_c)$  is the average of  $P_{w \times w}(\epsilon_\pi; w_1, w_2, n_c)$  across all possible weights. The possible combinations of  $w_1$  and  $w_2$  depend on the number of errors  $\epsilon_{CM}$  between  $\mathbf{f}_{B,1}^e$  and  $\mathbf{f}_{B,2}^e$ . If  $w_1$  and  $\epsilon_{CM}$  are known then the probability of  $w_2$  is determined by  $P_{w \times w}(w_2; w_1, \epsilon_{CM}, n_c)$ , because the error pattern can be considered as another binary vector of weight  $\epsilon_{CM}$ . With the probability of randomly selecting a binary vector of weight  $w_1$  equal to  $P_b(w_1; n_c, \frac{1}{2})$ , we obtain

$$P_{\epsilon_\pi}(\epsilon_\pi; P_e^{\text{ge}}, n_c) \stackrel{\text{def}}{=} \sum_{\epsilon_{CM}=0}^{n_c} \sum_{w_1=0}^{n_c} \sum_{w_2=0}^{n_c} P_{w \times w}(\epsilon_\pi; w_1, w_2, n_c) \times P_{w \times w}(w_2; w_1, \epsilon_{CM}, n_c) P_b(w_1; n_c, \frac{1}{2}) P_b(\epsilon_{CM}; n_c, P_e^{\text{ge}}), \quad (13)$$

Fig. 12 portrays the pmf of  $\epsilon_\pi$  at genuine comparisons obtained with (13) for different settings of  $P_e^{\text{ge}} \in \{\frac{1}{10}, \frac{3}{10}, \frac{1}{2}\}$  and  $n_c = \{31, 63\}$ . As a reference we use the case where  $\mathbf{e}_\pi$  is random binary vector with the pmf of its weight defined by the binomial pmf  $P_b(\epsilon_\pi; n_c, \frac{1}{2})$ . The figures show that the expected pmf of  $\epsilon_\pi$  is very close to the case of being random, if either  $P_e^{\text{ge}}$  and  $n_c$  increases the difference becomes smaller. If  $P_e^{\text{ge}} = \frac{1}{2}$  the pmf of  $\epsilon_\pi$  is equal to the case of being random.

Experimental results of the effects of the permutation randomization process, based on the same experimental setup

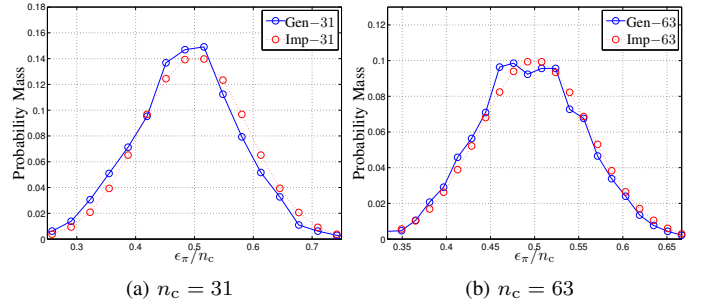


Fig. 13. The pmf of  $\epsilon_\pi = d_H(\mathbf{g}_{B,1}^e, \mathbf{g}_{B,2}^e)$  at both the genuine (Gen) and imposter (Imp) comparisons for (a)  $n_c = 31$  and (b)  $n_c = 63$  settings.

from Section V, are shown in Fig. 13. We observe that the pmf of  $\epsilon_\pi$  at genuine comparisons is close, however not equal, to the pmf at imposter comparisons, implying that it is difficult to distinguish a genuine comparison from an imposter comparison. These results confirm the theoretical expectations presented in Fig. 12. Note that due to the fewer number of genuine comparisons than imposter comparisons, the pmf for the genuine case is more noisy.

Finally, the cross-matching performance with the randomization process is estimated based on the score  $s_{CM}$  from (11) and the results are shown in Fig. 14. Fig. 14(a) depicts the pmf of  $s_{CM}$  at genuine (Gen) and imposter comparisons (Imp) for the  $n_c = \{31, 63\}$  settings. In contrast to the results in Fig. 9 we also include the scores larger than  $t_c$ . Both the genuine and imposter pmfs are very similar, hence no distinguishing performance can be extracted by the adversary. The cross-matching ROC curve for the  $n_c = \{31, 63\}$  settings are shown in Fig. 14(b). As expected, the ROC curves are close to the one of a random classifier whose ROC curve is defined by  $1 - \beta = \alpha$ . Because of the limited genuine comparisons, the ROC curve for the  $n_c = 63$  case looks to be a bit worse than the random classifier. Furthermore, the comparison between  $s_{CM}$  and  $\epsilon_{CM} = d_H(\mathbf{f}_{B,1}^e, \mathbf{f}_{B,2}^e)$  are portrayed in Fig. 14(c) and (d) for the  $n_c = 31$  and  $n_c = 63$  case, respectively. Due to the bit-permutation randomization process, the relationship between  $s_{CM}$  and  $\epsilon_{CM}$  (the straight line in the lower left quadrant), as observed in Fig. 10, no longer exists.

#### A. Inverting the Randomization Process

The randomization process and the bit-permutation matrix  $A_{\pi,1}$  stored as auxiliary data  $\text{AD}_3$  are considered as public. Hence, the adversary could apply the inverse on  $\text{AD}_2$ , namely  $A'_{\pi,1}\text{AD}_2$  with  $A'_{\pi,1} = A_{\pi,1}^{-1}$ , before applying the decodability attack on  $\text{AD}_\oplus$ . With the inverse process  $\text{AD}_\oplus$  becomes

$$\begin{aligned} \text{AD}_\oplus &= A'_{\pi,1}\text{AD}_{2,1} \oplus A'_{\pi,2}\text{AD}_{2,2} \\ &= A'_{\pi,1}(\mathbf{g}_{B,1}^e \oplus \mathbf{C}_1) \oplus A'_{\pi,2}(\mathbf{g}_{B,2}^e \oplus \mathbf{C}_2) \\ &= (A'_{\pi,1}A_{\pi,1}\mathbf{f}_{B,1}^e \oplus A'_{\pi,2}A_{\pi,2}\mathbf{f}_{B,2}^e) \oplus (A'_{\pi,1}\mathbf{C}_1 \oplus A'_{\pi,2}\mathbf{C}_2) \\ &= (\mathbf{f}_{B,1}^e \oplus \mathbf{f}_{B,2}^e) \oplus (A'_{\pi,1}\mathbf{C}_1 \oplus A'_{\pi,2}\mathbf{C}_2), \end{aligned} \quad (14)$$

with  $A'_{\pi,1}A_{\pi,1} = I$ . Note that due to the inverse operation, additional errors may be introduced by the fact that both code-words are permuted by two different bit-permutation matrices, namely  $(A'_{\pi,1}\mathbf{C}_1 \oplus A'_{\pi,2}\mathbf{C}_2) \in \mathcal{C}$ . The additional errors guar-

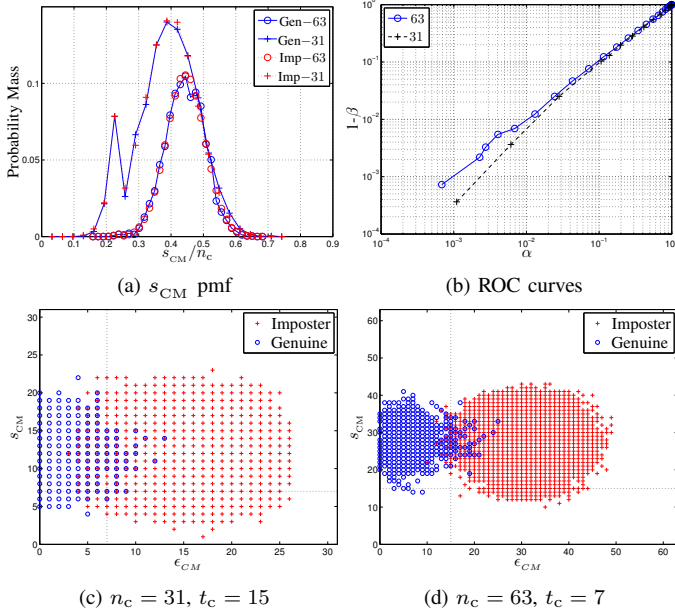


Fig. 14. (a) The pmf of  $s_{CM}$  and (b) the cross-matching ROC curve on logarithmic axes for  $n_c \in \{63, 31\}$ , and the comparison of  $s_{CM}$  against  $\epsilon_{CM} = d_H(\mathbf{f}_{B,1}^e, \mathbf{f}_{B,2}^e)$  for (c)  $n_c = 31$  and (d)  $n_c = 63$ .

antee that the cross-matching performance will be worse than the system performance. The only case where no errors are introduced is when  $(A'_{\pi,1}\mathbf{C}_1 \oplus A'_{\pi,2}\mathbf{C}_2) \in \mathcal{C}$ . We will show that this probability is very small, and thus there is a high probability that the cross-matching performance after taken the inverse is still worse than the system performance.

We will analyze this problem in two steps. First, given the codebook  $\mathcal{C}$  we estimate the probability of obtaining a binary vector of weight  $w$  from  $(A'_{\pi,1}\mathbf{C}_1 \oplus A'_{\pi,2}\mathbf{C}_2)$ , defined as  $P_{\pi-1}(w; \mathcal{C})$ . Hereafter, we estimate the probability that this binary vector is indeed a codeword, namely  $P_{\pi-1}(\mathcal{C})$ .

With  $W_{\mathcal{C}}$  defined as the set of possible weights  $w$  of the codewords from  $\mathcal{C}$  and the function  $N_{\mathcal{C}}(w)$  returning the number of codewords  $n_w$  with weight  $w$  with  $\sum_{w \in W_{\mathcal{C}}} N_{\mathcal{C}}(w) = |\mathcal{C}| = 2^{k_c}$ , the probability  $P_{\pi-1}(w; \mathcal{C})$  is equal to

$$\begin{aligned}
 P_{\pi-1}(w; \mathcal{C}) &\stackrel{\text{def}}{=} \mathcal{P}\{w = \|A'_{\pi,1}\mathbf{C}_1 \oplus A'_{\pi,2}\mathbf{C}_2\| \mid \\
 &\quad \forall \mathbf{C}_1, \mathbf{C}_2 \in \mathcal{C}, A_{\pi,1}, A_{\pi,2} \in \Pi\} \\
 &= \sum_{\substack{w_2 \in W_{\mathcal{C}} \\ w_1 \in W_{\mathcal{C}}}} \left\{ P_{w \times w}(w; w_1, w_2, n_c) \times \right. \\
 &\quad \left. \times \frac{N_{\mathcal{C}}(w_1)N_{\mathcal{C}}(w_2)}{2^{2k_c}} \right\}, \tag{15}
 \end{aligned}$$

where we take the sum, across all possible weights  $w_1$  and  $w_2$  of codewords  $\mathbf{C}_1$  and  $\mathbf{C}_2$ , of the product of  $P_{w \times w}(w; w_1, w_2, n_c)$  from (1) which is the probability that the XOR of two random binary vectors of weights  $w_1$  and  $w_2$  will lead to a binary vector of weight  $w$ , and  $\frac{N_{\mathcal{C}}(w_1)N_{\mathcal{C}}(w_2)}{2^{2k_c}}$  which is the probability of randomly selecting two codewords of weights  $w_1$  and  $w_2$  from  $\mathcal{C}$ . Fig. 15 illustrates  $P_{\pi-1}(w; \mathcal{C})$  for different  $n_c$  and  $[k_c, t_c]$  settings of the BCH ECC, compared with a binomial distribution  $P_b(w; n_c, \frac{1}{2})$ . Note that  $P_{\pi-1}(w; \mathcal{C})$  is very similar to the binomial probability except at weights zero and  $n_c$ ,

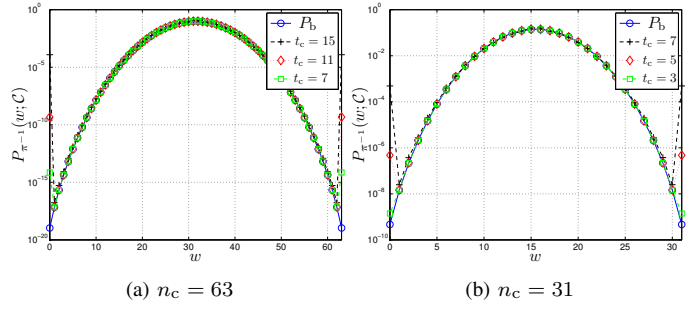


Fig. 15. The probability of obtaining a binary vector of weight  $w = \|\mathbf{C}_1 \oplus A_{\pi}\mathbf{C}_2\|$  given by  $P_{\pi-1}(w; \mathcal{C})$  from (15) for different  $n_c$  and  $t_c$  settings compared to a binomial distribution  $P_b(\epsilon; \pi; n_c, 0.5)$ .

where the difference increases when  $t_c$  increases. The weight,  $w = \|A'_{\pi,1}\mathbf{C}_1 \oplus A'_{\pi,2}\mathbf{C}_2\|$  is zero when both  $\|\mathbf{C}_1\|$  and  $\|\mathbf{C}_2\|$  are zero or  $n_c$ , or equal to  $n_c$  when one of the codewords has weight of zero and the other one  $n_c$ . Both cases have the probability  $P_{\pi-1}(0; \mathcal{C}) = P_{\pi-1}(n_c; \mathcal{C}) = \frac{2}{2^{2k_c}}$ .

With  $P_{\pi-1}(w; \mathcal{C})$  we can estimate the probability  $P_{\pi-1}(\mathcal{C})$  of the occurrence where no additional errors are introduced when the adversary applies the inverse, namely

$$\begin{aligned}
 P_{\pi-1}(\mathcal{C}) &\stackrel{\text{def}}{=} \mathcal{P}\{(A'_{\pi,1}\mathbf{C}_1 \oplus A'_{\pi,2}\mathbf{C}_2) \in \mathcal{C} \mid \\
 &\quad \forall \mathbf{C}_1, \mathbf{C}_2 \in \mathcal{C}, \forall A_{\pi,1}, A_{\pi,2} \in \Pi\} \tag{16} \\
 &= \sum_{w \in W_{\mathcal{C}}} P_{\pi-1}(w; \mathcal{C}) \frac{N_{\mathcal{C}}(w)}{\binom{n_c}{w}},
 \end{aligned}$$

where  $\frac{N_{\mathcal{C}}(w)}{\binom{n_c}{w}}$  is the probability that the binary vector of weight  $w$  is a codeword. Some examples of  $P_{\pi-1}(\mathcal{C})$  for different  $n_c$  and  $[k_c, t_c]$  settings are given in Table V. At smaller  $k_c$  settings  $P_{\pi-1}(\mathcal{C})$  is close to  $\frac{4}{2^{2k_c}}$ , which is the probability of only selecting codewords of either weight zero or  $n_c$ . For those cases, no additional errors are introduced by  $A'_{\pi,1}\mathbf{C}_1 \oplus A'_{\pi,2}\mathbf{C}_2$ . The probability  $P_{\pi-1}(\mathcal{C})$  can be reduced even further by removing these two codewords from the original codebook, thus obtaining the codebook  $\mathcal{C} \setminus \{0, n_c\}$ . The probability is then given by  $P_{\pi-1}(\mathcal{C} \setminus \{0, n_c\})$  and its value for the same  $n_c$  and  $[k_c, t_c]$  settings are given in Table V. At smaller  $k_c$  values,  $P_{\pi-1}(\mathcal{C} \setminus \{0, n_c\})$  is significantly smaller than  $P_{\pi-1}(\mathcal{C})$ . Hence, in order to be more robust against the inverse of the bit-permutation process prior to the decodability attack, it is recommended not to use the codewords of weight zero or  $n_c$ . The drawback is that the key space is reduced to  $2^{k_c} - 2$ , which becomes negligible for larger  $k_c$  values. However at larger  $k_c$  values both  $P_{\pi-1}(\mathcal{C})$  and  $P_{\pi-1}(\mathcal{C} \setminus \{0, n_c\})$  converge to each other. From the results of Fig. 15, we observe that at larger  $k_c$  values it holds that  $P_{\pi-1}(w; \mathcal{C}) \approx P_b(w; n_c, \frac{1}{2})$ , consequently (16) becomes

$$\begin{aligned}
 P_{\pi-1}(\mathcal{C}) &= \sum_{w \in W_{\mathcal{C}}} P_{\pi-1}(w; \mathcal{C}) \frac{N_{\mathcal{C}}(w)}{\binom{n_c}{w}} \\
 &\approx \sum_{w \in W_{\mathcal{C}}} P_b(w; n_c, \frac{1}{2}) \frac{N_{\mathcal{C}}(w)}{\binom{n_c}{w}} \\
 &= \sum_{w \in W_{\mathcal{C}}} \frac{\binom{n_c}{w} N_{\mathcal{C}}(w)}{2^{n_c} \binom{n_c}{w}} \\
 &= \frac{1}{2^{n_c}} \sum_{w \in W_{\mathcal{C}}} N_{\mathcal{C}}(w) \\
 &= 2^{k_c - n_c} \tag{17}
 \end{aligned}$$

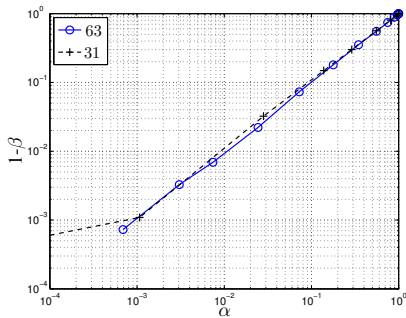


Fig. 16. The cross-matching ROC curve when applying the decodability attack after inverting the randomization process on logarithmic axes for the  $n_c \in \{63, 31\}$  settings.

which is the probability of randomly guessing a codeword from  $\mathcal{C}$ . Empirical results shown in Fig. 16 confirm that inverting the randomization process prior to applying the decodability attack does not give the adversary an advantage when using the decodability attack, because the ROC curve is still close to random.

### B. Ineffectiveness of the Noise-Addition Randomization Method

We will show that not all randomization processes will work. For example, taking the XOR of  $\mathbf{f}_B^e$  with a random bit pattern  $\delta$ , hence obtaining  $\mathbf{g}_B^e = \mathbf{f}_B^e \oplus \delta$  does not work, because this randomization process is fully reversible. When taking the XOR between  $\text{AD}_{2,1}$  and  $\text{AD}_{2,2}$  we obtain

$$\begin{aligned} \text{AD}_{2,1} \oplus \text{AD}_{2,2} &= (\mathbf{g}_{B,1}^e \oplus \mathbf{C}_1) \oplus (\mathbf{g}_{B,2}^e \oplus \mathbf{C}_2) \\ &= ((\mathbf{f}_{B,1}^e \oplus \delta_1) \oplus (\mathbf{f}_{B,2}^e \oplus \delta_2)) \oplus (\mathbf{C}_1 \oplus \mathbf{C}_2) \\ &= (\delta_1 \oplus \delta_2) \oplus (\mathbf{f}_{B,1}^e \oplus \mathbf{f}_{B,2}^e) \oplus (\mathbf{C}_1 \oplus \mathbf{C}_2) \end{aligned} \quad (18)$$

Hence, it is sufficient to take the XOR of the auxiliary data  $\text{AD}_2$  with the publicly known bit pattern  $\delta$  prior to applying the decodability attack, namely

$$\begin{aligned} (\delta_1 \oplus \text{AD}_{2,1}) \oplus (\delta_2 \oplus \text{AD}_{2,2}) &= (\delta_1 \oplus \delta_2) \oplus (\text{AD}_{2,1} \oplus \text{AD}_{2,2}) \\ &= (\mathbf{f}_{B,1}^e \oplus \mathbf{f}_{B,2}^e) \oplus (\mathbf{C}_1 \oplus \mathbf{C}_2), \end{aligned} \quad (19)$$

because  $(\delta_1 \oplus \delta_2) \oplus (\delta_1 \oplus \delta_2)$  cancel each other out. Hence, the adversary obtains the same error pattern  $(\mathbf{f}_{B,1}^e \oplus \mathbf{f}_{B,2}^e) \oplus (\mathbf{C}_1 \oplus \mathbf{C}_2)$  with which cross-matching is possible as shown in Section III.

### C. Effect on the Exhaustive Search Attack

In Section III we discussed both the decodability attack and the attacks based on exhaustive searches. With the bit-

TABLE V  
THE PROBABILITY  $P_{\pi^{-1}(\mathcal{C})}$  AND  $P_{\pi^{-1}(\mathcal{C} \setminus \{0, n_c\})}$  FOR DIFFERENT SETTINGS OF  $n_c$  AND  $[k_c, t_c]$ .

$n_c = 31$			
$[k_c, t_c]$	[6, 7]	[11, 5]	[16, 3]
$P_{\pi^{-1}(\mathcal{C})}$	$9.7660 \cdot 10^{-4}$	$1.9103 \cdot 10^{-6}$	$3.0521 \cdot 10^{-5}$
$P_{\pi^{-1}(\mathcal{C} \setminus \{0, n_c\})}$	$2.8424 \cdot 10^{-8}$	$9.5271 \cdot 10^{-7}$	$3.0517 \cdot 10^{-5}$
$n_c = 63$			
$[k_c, t_c]$	[7, 15]	[16, 11]	[24, 7]
$P_{\pi^{-1}(\mathcal{C})}$	$2.4414 \cdot 10^{-4}$	$9.3133 \cdot 10^{-10}$	$1.8332 \cdot 10^{-12}$
$P_{\pi^{-1}(\mathcal{C} \setminus \{0, n_c\})}$	$1.3555 \cdot 10^{-17}$	$7.1052 \cdot 10^{-15}$	$1.8190 \cdot 10^{-12}$

permutation process we reduced the effectiveness of the decodability attack, however both exhaustive attack methods still exist. With the bit-permutation process, the exhaustive search type of Case 1, where both the auxiliary data  $\text{AD}_2$  and Pseudonymous Identifier PI are available, remains unchanged. By guessing the codeword from PI, the permuted binary vector  $\mathbf{g}_B^e$  can be computed from which we can obtain  $\mathbf{f}_B^e$  by inverting the bit-permutation process with  $A_\pi$ . However the exhaustive search type of Case 2, where only the auxiliary data is available, changes. The exhaustive search attack without the bit-permutation process as discussed in Section III-A has to search for a single codeword from the codebook  $\mathcal{C}$  leading to the smallest distance score  $s_{\text{CM}} = \min_{\mathbf{C} \in \mathcal{C}} \|\text{AD}_\oplus \oplus \mathbf{C}\|$  with an average effort around  $\approx 2^{k_c-1}$ . However, once the codeword was found there was still an ambiguity about the binary vector  $\mathbf{f}_B^e$  of  $2^{k_c}$  possibilities. With the bit-permutation process, the XOR of the inverse of the auxiliary data of (2) becomes

$$\text{AD}_\oplus = (\mathbf{f}_{B,1}^e \oplus \mathbf{f}_{B,2}^e) \oplus (A'_{\pi,1} \mathbf{C}_1 \oplus A'_{\pi,2} \mathbf{C}_2), \quad (20)$$

where the linear property of the ECC no longer holds as in (2). Instead of searching the codebook  $\mathcal{C}$  only once, all combinations of the permuted codewords  $A'_{\pi,1} \mathbf{C}_1 \oplus A'_{\pi,2} \mathbf{C}_2$  with known bit-permutation matrices has to be searched leading to the smallest distance score  $s_{\text{CM}} = \min_{\mathbf{C}_1, \mathbf{C}_2 \in \mathcal{C}} \|\text{AD}_\oplus \oplus A'_{\pi,1} \mathbf{C}_1 \oplus A'_{\pi,2} \mathbf{C}_2\|$ . Thus, the effort has significantly increased towards  $\approx 2^{2k_c-1}$ . However, once the codewords  $\mathbf{C}_1$  and  $\mathbf{C}_2$  have been found, the binary vector  $\mathbf{f}_B^e$  is fully known. Hence, there is a trade-off between the case where cross-matching with the effortless decodability attack is possible with protection of the binary vectors or the case where cross-matching matching is possible with a significantly increased effort of  $2^{2k_c-1}$  but revealing the binary vectors at a successful cross-match.

## VII. CONCLUSIONS

We analyzed the cross-matching performance of the auxiliary data  $\text{AD}_2$  of the Fuzzy Commitment Scheme (FCS). We showed two attacks based on an exhaustive search, resulting in a significant attack effort, as well as a recently introduced attack requiring only a single decoding operation of the ECC, known as the decodability attack. Both attacks have the same cross-matching performance. To the best of our knowledge, the decodability attack was first presented in [14] and theoretically analyzed in [15]. We extended this theoretical analysis and showed the relationship between the balanced template protection system where  $N_v = N_e$  and the cross-matching performance. The FMR at cross-matching is  $2^{k_c}$  larger than the FMR of the system, where  $k_c$  is the key size of the ECC. On the contrary, the FNMR at cross-matching is smaller than the FNMR of the system. However, the difference significantly decreases for larger  $n_c$  values. When comparing both the FMR and FNMR in a ROC curve, we showed that the cross-matching performance is clearly worse than the system performance. We empirically validated the presented theoretical analysis using real biometric data from the MCYT fingerprint database. *Concluding, designing a balance template protection system with  $N_v = N_e$  guarantees*

that the cross-matching performance is always worse than the system performance itself.

Ideally, the cross-matching performance should be close to random. We provided a solution based on a bit-permutation randomization process that reduces the cross-matching performance of the decodability attack very close to random under the assumption that independent samples are taken for each application. During the enrolment phase, a random bit-permutation matrix is generated and used to permute the binary vector prior to creating the auxiliary data. We can consider the bit-permutation matrix of the randomization process to be publicly known because we have shown that the cross-matching performance is still close to random even when inverting the bit-permutation randomization process.

We showed the following trade-off. Without the proposed bit-permutation randomization process the decodability cross-matching attack is effortless, however without revealing the enrolled binary vectors. With the bit-permutation randomization process, the decodability cross-matching attack is neutralized however cross-matching based on exhaustive search is still possible. The effort of the exhaustive search increased towards  $2^{2k_c-1}$ , instead of  $2^{k_c}$  when the bit-permutation randomization process is not applied. However, the effort increase is obtained with a drawback, namely revealing the enrolled binary vectors at a successful cross-match.

## REFERENCES

- [1] "ISO/IEC JTC1 SC27. FCD 24745 - information technology - security techniques - biometric template protection," 2010.
- [2] A. Juels and M. Wattenberg, "A fuzzy commitment scheme," in *6th ACM Conference on Computer and Communications Security*, November 1999, pp. 28–36.
- [3] E. J. C. Kelkboom, B. Gökberk, T. A. M. Kevenaar, A. H. M. Akkermans, and M. van der Veen, "'3D face': Biometric template protection for 3D face recognition," in *Intl. Conf. on Biometrics*, Seoul, South Korea, August 2007, pp. 566 – 573.
- [4] T. A. M. Kevenaar, G.-J. Schrijen, A. H. M. Akkermans, M. van der Veen, and F. Zuo, "Face recognition with renewable and privacy preserving binary templates," in *4th IEEE workshop on AutoID*, Buffalo, New York, USA, October 2005, pp. 21–26.
- [5] J.-P. Linnartz and P. Tuyls, "New shielding functions to enhance privacy and prevent misuse of biometric templates," in *4th Int. Conf. on AVBPA*, 2003, pp. 393 – 402.
- [6] E.-C. Chang and S. Roy, "Robust extraction of secret bits from minutiae," in *Int. Conf. on Biometrics*, Seoul, South Korea, August 2007, pp. 750–759.
- [7] Y. Dodis, L. Reyzin, and A. Smith, "Fuzzy extractors: How to generate strong secret keys from biometrics and other noisy data," in *Advances in Cryptology - Eurocrypt 2004, LNCS 3027*, 2004, pp. 532 – 540.
- [8] A. Juels and M. Sudan, "A fuzzy vault scheme," *Designs, Codes and Cryptography*, vol. 38, no. 2, pp. 237–257, February 2006.
- [9] K. Nandakumar, A. K. Jain, and S. Pankanti, "Fingerprint-based fuzzy vault: Implementation and performance," *IEEE Transactions on Information Forensics and Security*, vol. 2, no. 4, pp. 744 – 757, December 2007.
- [10] N. K. Ratha, S. Chikkerur, J. H. Connell, and R. M. Bolle, "Generating cancelable fingerprint templates," *IEEE Transactions on Pattern Analysis and Machine Intelligence*, vol. 29, no. 4, pp. 561 – 572, April 2007.
- [11] W. J. Scheirer and T. E. Boult, "Cracking fuzzy vaults and biometric encryption," in *Proceedings of Biometric Symposium*, Baltimore, MD, September 2007.
- [12] K. Nandakumar, A. Nagar, and A. K. Jain., "Hardening fingerprint fuzzy vault using password." in *Proceedings of Second International Conference on Biometrics*, Seoul, South Korea, August 2007, pp. 927 – 937.
- [13] J. Bringer, H. Chabanne, and B. Kindarji, "The best of both worlds: Applying secure sketches to cancelable biometrics," in *Science of Computer Programming*, October 2008.
- [14] F. Carter and A. Stoianov, "Implications of biometric encryption on wide spread use of biometrics," in *EBF Biometric Encryption Seminar*, Amsterdam, The Netherlands, June 2008. [Online]. Available: [http://www.eubiometricsforum.com/pdfs/be/BE-Carter\\_Stoianov.pdf](http://www.eubiometricsforum.com/pdfs/be/BE-Carter_Stoianov.pdf)
- [15] K. Simoens, P. Tuyls, and B. Preneel, "Privacy weaknesses in biometric sketches," in *Proceedings of the 2009 IEEE Symposium on Security and Privacy*. IEEE Computer Society, 2009.
- [16] P. Tuyls, A. H. M. Akkermans, T. A. M. Kevenaar, G.-J. Schrijen, A. M. Bazen, and R. N. J. Veldhuis, "Practical biometric authentication with template protection," in *5th International Conference, AVBPA*, Rye Brook, New York, July 2005.
- [17] J. Breebaart, C. Busch, J. Grave, and E. Kindt, "A reference architecture for biometric template protection based on pseudo identities," in *BIOSIG*, Darmstadt, Germany, September 2008.
- [18] J. Daugman, "The importance of being random: statistical principles of iris recognition," *Pattern Recognition*, vol. 36, no. 2, pp. 279–291, 2003.
- [19] J. Ortega-Garcia, J. Fierrez-Aguilar, D. Simon, J. Gonzalez, M. Faundez-Zanuy, V. Espinosa, A. Satue, I. Hernaez, J. J. Igarza, C. Vivaracho, D. Escudero, and Q. I. Moro, "MICYT baseline corpus: A bimodal biometric database," in *IEE Proc. Vision, Image and Signal Processing, Special Issue on Biometrics on the Internet*, December 2003, pp. 395 – 401.
- [20] M. van der Veen, A. Bazen, T. Ignatenko, and T. Kalker, "Reference point detection for improved fingerprint matching," in *Proceedings of SPIE*, 2006, p. 60720G.160720G.9.
- [21] A. M. Bazen and R. N. J. Veldhuis, "Likelihood-ratio-based biometric verification," *Circuits and Systems for Video Technology, IEEE Transactions on*, vol. 14, no. 1, pp. 86–94, 2004.